Uncertainties associated with the surface texture of ice particles in satellite-based retrieval of cirrus clouds: Part II. Effect of particle surface roughness on retrieved cloud optical thickness and effective particle size

Ping Yang, Gang Hong, and George W. Kattawar

Texas A&M University, College Station, TX 77843

Patrick Minnis and Yong X. Hu

NASA Langley Research Center, Hampton, VA 23681

For publication in

IEEE Transactions on Geoscience and Remote Sensing

Corresponding author address: Dr. Ping Yang, Department of Atmospheric Sciences, Texas A&M University, College Station, TX 77843; Tel: 979-845-4923.

Email: pyang@ariel.met.tamu.edu

Abstract

The effect of the surface roughness of ice crystals on the retrieval of the optical and microphysical properties of cirrus clouds is investigated. The simplified ray-tracing technique reported in the first part of this study (hereafter, Part I) is employed to compute the single-scattering properties of hexagonal columns with maximum dimensions ranging from 2 to 3500 μm with a size-bin-resolution of 2 μm at wavelengths 0.86 and 2.13 μm. The scattering properties of these particles are then averaged over 18 particle size distributions whose effective particle radii (r_e) range from 5 to 90 μm. The single-scattering properties of ice clouds are strongly sensitive to surface roughness condition. Look-up tables built for the correlation between the bi-directional reflectances at wavelengths 0.86 and 2.13 μm with different roughness conditions are used to retrieve ice cloud optical thickness and effective particle size over oceans. Pronounced differences are noticed for the retrieved cirrus cloud optical thickness and effective particle sizes in conjunction with different surface roughness conditions. The values of the retrieved cirrus cloud optical thickness in the case of the rough surface are generally smaller than their counterparts associated with smooth surface conditions. The effect of surface roughness on the retrieved effective particle radii is not pronounced for slight and moderate roughness conditions. However, when the surfaces of ice crystals are substantially rough, the retrieved effective radii associated with roughened particles are larger and smaller than their smooth surface counterparts for large ($r_e > 50$ μm) and small ($r_e < 35$ μm) ice crystals, respectively, whereas the effect of surface roughness on the retrieved effective radii shows a non-monotonic feature for moderate particle sizes ($35\ \mu m < r_e < 50 \mu m$). In general, the dominant effect of surface roughness on cloud

property retrievals is to decrease the retrieved optical thickness and to increase the retrieved effective particle size in comparison with their counterparts in the case of smooth ice particles.

1. Introduction

The scattering characteristics typical for pristine ice crystals with smooth surface and basic hexagonal structures either in a form of single particles or aggregates are the halo peaks in the angular distribution of scattered radiation. As articulated by Mishchenko et al. [1] on the basis of the observations reported in the literature, halos are not often seen in the atmosphere and the phase functions associated with ice clouds might be featureless with no pronounced halo peaks. One of the mechanisms responsible for the featureless phase function might be the surface distortion or roughness of ice crystals [1-3]. Ice crystals may have rough surfaces due to evaporation/sublimation [4,5] or riming process [6]. Rolland et al. [7] studied the sensitivity of retrieved optical thickness and effective particle size to of ice particle surface roughness through its impact on the single-scattering properties. However, in their study, the roughness condition is not quantitatively specified. Thus, there is a need to further investigate the effect of the surface roughness on the retrieval of the optical and microphysical properties of ice clouds. During the past 20 years, numerous techniques have been developed to infer the radiative and microphysical properties of ice clouds from the polarimetric or scalar radiometric measurements made by various satellite-borne sensors [8-15]. During the night, three infrared bands centered at 8.5, 11, and 12 μm in the thermal infrared window region are often used [16-18]. Note that the retrieval techniques based on the thermal infrared radiation are also applicable to the retrievals of cloud properties during daytime. The correlation of the brightness temperature difference (BTD) between 11 and 12 μm ($BTD_{11\text{-}12\mu m}$) and the brightness temperature (BT) at 11 μm ($BT_{11\mu m}$), i.e., the relationship between $BTD_{11\text{-}12\mu m}$ and $BT_{11\mu m}$, contains rich information for simultaneously retrieving the optical thicknesses and effective particle sizes of ice clouds. The sensitivity of the bulk radiative properties of a cloud to the optical and microphysical properties of the cloud also exists in the correlation between the BTD between 8.5 and 12 μm (or 8.5 and

11 μm) and the BT at 8.5 μm, which can also be useful for retrieving cloud optical thickness and effective particle size. The technical details of this approach can be found in [16] and the references cited therein. Furthermore, the emissivity of ice clouds in the infrared channels of the thermal infrared window region can be used to infer the effective particle size [19,20]. For the thermal infrared radiation associated with ice clouds, the spectral signatures are determined primarily by the absorption properties of the clouds, which are not sensitive to the detailed features of the scattering phase function. Additionally, the phase functions of ice crystals at infrared wavelengths may be smooth or featureless due to the absorption of these particles, which may have little sensitivity to the textures of ice crystal surfaces. For these reasons, the effect of the surface roughness of ice particles on the retrieval of cloud properties from the infrared spectral information may be insignificant. Thus, the present study focuses on the effect of the surface roughness on the retrieval of cloud properties based on visible and near-infrared radiation.

Under daytime conditions, a popular approach for a simultaneous retrieval of the optical thicknesses and effective particle sizes is the bi-spectral method developed by Nakajima and King [21]. The physical basis of this method is that the reflectance under cloudy conditions at a non-absorbing band (e.g., a band centered at 0.66 μm) is sensitive primarily to the optical thickness whereas the reflectance of a cloud at an absorbing band (e.g., a band centered at 2.13 μm) is sensitive to the effective particle size. The comparison of a pair of measured reflectances at 0.66 and 2.13 μm with a pre-computed correlation of the 2.13-μm and 0.66-μm reflectances provides a straightforward approach for estimating the optical thickness and effective particle sizes. The pre-computed correlation of the 2.13- and 0.66-μm reflectances, usually known as a look-up library used for implementing the retrieval algorithm, is critical to the correctness of the retrieval results. This bi-spectral method has been used in the operational cloud retrievals based on the Moderate Resolution Imaging Spectroradiometer (MODIS) measurements [22,23]. In

practice, in the MODIS operational cloud retrieval algorithm the 0.65-, 0.86-, and 1.24-μm bands are selected as the non-absorbing bands in the bi-spectral algorithm for use over land, ocean, and ice/snow surfaces, respectively. The 2.13-μm band is selected as the primary absorbing band for implementing the bi-spectral algorithm. Furthermore, a combination of the 1.64 or 3.78 μm band and a non-absorbing band (e.g., 0.65, 0.84, or 1.24-μm band) can quantify the deviations from those retrieved on the basis of a combination of the 2.13-μm band and a nonabsorbing band (e.g., the 0.65-μm band) [23]. In the development of the MODIS look-up library for the bidirectional reflectances of ice clouds [24,25], all ice crystal habits except aggregates are assumed to have smooth surfaces. The present study is intended to investigate the effect of the surface roughness of ice crystals on the retrieval of the optical and microphysical properties of ice clouds using the visible and near-infrared solar radiation reflected by ice clouds on the basis of the bi-spectral method developed by Nakajima and King [21] and the data acquired by the MODIS instrument aboard the *Terra* satellite platform.

2. Single-scattering properties of roughened ice particles

For simplicity in the present sensitivity study, ice crystals are assumed to be randomly oriented hexagonal columns with roughened surfaces. The simplified ray-tracing technique described in Part I [26] is employed to compute the single-scattering properties of ice crystals, as it can approximately account for the effect of surface roughness on the single-scattering properties of roughened ice particles. Following Yang and Liou [3], the probability density function (PDF) for the spatial orientations of the rough surface facets of an ice crystal is specified by the first order Gram-Charlier or the two-dimensional Gaussian distribution [27] as follows:

$$\xi(z_\alpha, z_\beta) = \frac{1}{\pi\sigma^2}\exp\left[-(z_\alpha^2 + z_\beta^2)/\sigma^2\right], \tag{1}$$

where the function ξ indicates the PDF. The parameters z_α and z_β indicate the slopes of a facet of the roughened surface along two orthogonal directions specified in terms of two unit vectors $\hat{\alpha}$ and $\hat{\beta}$ that are tangential to the overall averaged surface position (i.e., the case of smooth surface). Specifically, the parameters z_α and z_β can be defined as follows [3]:

$$z_\alpha = (\mu^{-2} - 1)^{1/2} \cos\varphi, \tag{2a}$$

$$z_\beta = (\mu^{-2} - 1)^{1/2} \sin\varphi, \tag{2b}$$

$$\mu = \cos\theta, \tag{2c}$$

where θ and φ are the zenith and azimuthal angles of the normal of a roughness facet, respectively, which are specified with respect to the normal of the corresponding smooth surface. The definition of the azimuthal plane of $\varphi = 0$ is arbitrary as long as the definition is kept consistent in the ray-tracing calculation. In Eq. (1), the degree of surface roughness is specified in terms of the parameter σ. As an example, Figure 1 shows $\xi(z_\alpha, 0)$ for three roughness conditions, $\sigma = 0.01,\ 0.1$ and 1.0. Note that we select $z_\beta = 0$ in Fig.1 to avoid using a three-dimensional illustration. It is evident from Fig.1 that the width of the distribution of the parameter z_α is proportional to σ. As the degree of surface roughness increases with the widths of the distributions of z_α and z_β, the parameter σ well defines how rough ice crystal surface is. Specifically, the larger the parameter σ is, the rougher the surface is.

In the ray-tracing calculation, the normal direction of ice crystal surface is locally titled in a random way to represent a realization of a rough surface facet for each reflection and refraction event [2,3], as described in Part I [26]. In practice, the Monte

Carlo method can be used to specify the orientation of the normal direction of the facet on the basis of Eqs. (1) and (2), as described in detail by Yang and Liou [3]. Most recently, Shcherbakov et al. [28] developed a new approach based on the Weibull distribution for the PDF of the rough surface facets, which can also be used to compute the single-scattering properties of roughen ice crystals.

Figure 2 shows the phase functions at a wavelength of 0.66 μm for randomly oriented compact hexagonal ice crystals ($2a/L$=100 μm/100 μm), hexagonal columns ($2a/L$=100 μm/300 μm), and hexagonal plates ($2a/L$=300 μm/100 μm), where a and L indicate the semi-width of the cross section and length of an ice crystal, respectively. The refractive index of ice at this wavelength is $1.3078 + i1.66 \times 10^{-8}$. Four roughness conditions with $\sigma = 0$ (smooth surface), $\sigma = 0.01$ (slight roughness), $\sigma = 0.1$ (moderate roughness), and $\sigma = 1.0$ (deep roughness) are imposed in the computation. The left panels in Fig. 2 show the phase function values at scattering angles ranging from 0° to 180°, and the right panels in Fig. 2 zoom in on the phase functions in forward directions from 0° to 2°. The phase functions of randomly oriented hexagonal ice crystals with smooth surfaces (i.e., $\sigma = 0.0$) have been extensively discussed in the literature [2, 3 and references cited therein], and those discussions should not be recaptured here. For the slight roughness condition ($\sigma = 0.01$), the effect of the surface roughness is to decrease the backscattering intensity. Additionally, the 22° peak is slightly reduced, but the 46° halo peak is substantially diminished. For the moderate roughness condition ($\sigma = 0.1$), the surface roughness substantially smoothes out the 22° and 46° halo peaks and diminishes the backscattering. For the deep roughness condition ($\sigma = 1.0$), the phase functions are essentially featureless. These features of the scattering phase functions of roughened ice

crystals are consistent with those reported in the literature (e.g., [2,3]). Furthermore, it is evident from the results shown in Fig. 2 that the asymmetry factors for roughened particles are smaller than their smooth-surface counterparts. The asymmetry factors for the columns and plates with rough surfaces decrease with the increase of the degree of the surface roughness. On the contrary, the asymmetry factor for the compact particles with unit aspect ratio ($2a/L$=100 μm/100 μm) slightly increases with the increase of the degree of surface roughness in the case of $\sigma = 0.01,\ 0.1$ and 1 although the asymmetry factors for the roughened particles are still smaller than their corresponding smooth-surface counterpart.

It is evident from Fig. 2 that the effect of the surface roughness on the single-scattering properties of the particle also depends on the aspect ratios of the ice crystals. To further illustrate this feature of the surface roughness effect, Fig. 3 shows the comparison of the asymmetry factors as functions of the aspect ratio for σ = 0.00, 0.01, 0.10, and 1.00 (upper panel in Fig. 3) and for σ = 0.00, 0.0015, 0.0025, and 1.00 (lower panel in Fig. 3). To specify the sizes of ice crystals in the calculation, we let the surface areas of ice crystals with various aspect ratios be the same as that of an ice crystal whose size is $a/L = 60\mu m/300\mu m$. As shown in Fig. 3, the values of the asymmetry factor are the lowest when the aspect ratio is approximately 1 regardless of the roughness conditions. This feature of the variation of the asymmetry factor versus the aspect ratio has been reported by Macke and Mishchenko [29], Grenfell et al. [30] and Fu [31] in the case of smooth ice crystals. It is also evident from Fig. 3 that the effect of surface roughness on the asymmetry increases with the deviation of aspect ratio from 1 in both

cases of columns (i.e., $2a/L < 1$) and plates (i.e., $2a/L > 1$). This feature is especially pronounced in the comparison of the results associated with $\sigma = 0.0$ and 1.0.

When $2a/L < 0.7$ or $2a/L > 2$, the asymmetry factor monotonically decreases with the increase of σ (i.e., the degree of surface roughness) for a given aspect ratio. When $2a/L \approx 1$, the effect of surface roughness on the asymmetry factor is minimum; and the variation of the asymmetry factor versus σ is not monotonic, as is evident from the zoomed-in curves in the upper and lower panels of Fig. 3. The physical mechanism associated with the non-monotonic variation of the asymmetry factor versus σ in the case of $2a/L \approx 1$ is not clear at this point. However, in this case the maximum differences of the asymmetry factors for six roughness conditions (σ=0.00, 0.0015, 0.0025, 0.01, 0.10 and 1) are on the order of 0.005 in the aspect ratio region near $2a/L = 1$. The features of the roughness effect showed in Fig. 3 have an important implication to practical application. Small ice crystals (<50 μm) in cirrus clouds tend to be compact ice crystals. Thus, the effect of surface roughness on the optical properties of these particles is much smaller in comparison with the case for large particles shaped in either plates or columns.

Figure 4 shows the asymmetry factors as functions of the maximum dimensions of columns with four different surface roughness conditions (σ = 0.00, 0.01, 0.10, and 1.00). The aspect ratio is *2a/L* = 1/3. The wavelength and refractive index for Fig. 4 are the same as those for Figs. 2 and 3. For ice crystals smaller than approximately 20 μm, the asymmetry factors increase with increasing maximum dimensions. For larger ice crystals, the asymmetry factors tend to reach their asymptotic values. It is evident from Fig. 4 that the asymmetry factors are strongly sensitive to surface roughness at this aspect

ratio. Specifically, with increasing surface roughness, the asymmetry factors substantially decrease.

For remote sensing applications, the single-scattering properties of ice crystals must be averaged over size distributions. For a given size distribution, we assume that the aspect ratios of an ice crystal population can be specified by the formula reported by Yang et al. [32] as follows:

$$2a/L = \begin{cases} 1, & L \le 40\ \mu m, \\ \exp[-0.017835(L-40)], & 40 < L \le 50\ \mu m, \\ 5.916/L^{1/2}, & L > 50\ \mu m. \end{cases} \tag{3}$$

For a given size distribution, the bulk single-scattering properties of ice crystals can be obtained, e.g., for the phase function P, as follows:

$$P(\theta) = \frac{\int_{D_{\min}}^{D_{\max}} P(\theta,D) C_{sca}(D) n(D) dD}{\int_{D_{\min}}^{D_{\max}} C_{sca}(D) n(D) dD}, \tag{4}$$

where D is the maximum dimension of an ice crystal, n indicates the size distribution of ice crystals, and C_{sca} is the scattering cross section of an ice crystal with a maximum dimension of D. To be consistent with the definition of the effective particle size in the MODIS operational cloud retrieval, the effective particle radius is defined following King et al. [24] and references cited therein as follows:

$$r_e = \frac{3}{4} \frac{\int_{D_{\min}}^{D_{\max}} V(D) n(D) dD}{\int_{D_{\min}}^{D_{\max}} A(D) n(D) dD}, \tag{5}$$

where V and A are the volume and projected area of an ice crystal with a maximum dimension of D, respectively. As pointed out by King et al. [24], the definition in Eq. (5)

is consistent with the definition given by Hansen and Travis [33] in the case of spherical water droplets.

3. Effect of Surface Roughness on Retrieving Cloud properties

To investigate the influence of ice crystal surface roughness on cloud property retrievals, the single-scattering properties are computed from an improved geometric optics method [33] for ice crystals with maximum dimensions ranging from 2 to 3500 μm with a size-bin resolution of 2 μm. The bulk scattering properties are then derived by averaging the single-scattering properties over 18 particle size distributions with effective radii varying from $r_e = 5$ to $r_e = 90$ μm. The Gamma distribution (e.g., [35]) is assumed for the size distributions of ice crystals, given as follows:

$$n(D) = N_0 D^{\mu} \exp(-\frac{b + \mu + 0.67}{D_m} D), \tag{6}$$

where N_0 is the intercept, μ is the dispersion usually ranging from 0 to 2 and is assumed to be 2 in this study, where D_m is the median of the distribution of D. The values of parameter b are 2.1 and 2.3 for the tropical and midlatitude ice clouds, respectively [36]. Their mean value $b = 2.2$ is used in this study.

Figure 5 shows the phase functions at 0.86 and 2.13 μm for four surface roughness conditions, σ = 0.00, 0.01, 0.10, and 1.00, with an effective particle radius of 30 μm. Lookup tables of the correlation between the 0.86- and 2.13-μm reflectances for the four surface roughness conditions (i.e., σ = 0.00, 0.01, 0.10, and 1.00) with a solar zenith angle of 30°, a satellite zenith angle of 0°, and a relative azimuth angle of 90° are also shown in Fig. 5. The phase functions in the case of smooth surafce show distinct scattering peaks. The phase functions are smoothed as the degree of surface roughness

increases. Moreover, ice crystals without surface roughness scatter more energy in backscattering directions than their roughened counterparts. The look-up tables for different roughness conditions also show pronounced differences that could result in differences in the retrieved ice cloud optical thickness and effective particle size.

Look-up tables of band reflectances as functions of solar zenith angle, satellite zenith angle, relative azimuth angle, ice cloud optical thickness, and effective particle size for four roughness conditions, σ = 0.00, 0.01, 0.10, and 1.00, are used to estimate the optical thickness and effective particle size of ice clouds by minimizing the following cost function:

$$\chi^2 = [R^m_{0.86}(\theta_0,\ \theta,\ \phi)\ -\ R^l_{0.86}(\tau,\ r_e;\ \theta_0,\ \theta,\ \phi)]^2 + [R^m_{2.13}(\theta_0,\ \theta,\ \phi)\ -\ R^l_{2.13}(\tau,\ r_e;\ \theta_0,\ \theta,\ \phi)]^2, \quad (7)$$

where $R^m_{0.86}$ and $R^m_{2.13}$ are the satellite measured bidirectional reflectances at the 0.86- and 2.13-μm bands, respectively, and $R^l_{0.86}$ and $R^l_{2.13}$ are the bidirectional reflectances in the pre-calculated lookup table for ice clouds. The retrieved τ and D_e can then be obtained from the preceding minimization procedure.

Figure 6 shows the retrieved results based on the MODIS measurements. Specifically, a MODIS granule over the Indian Ocean at 04:35 UTC on 22 June 2006 is used in the retrieval. The RGB composite image based on MODIS band 4 (0.55 μm), 3 (0.47 μm), and 1 (0.65 μm) shows that clouds essentially cover the entire region of this granule. The properties of the ice clouds in the region included by the red box in Fig. 6 are retrieved. Moreover, the retrieval is conducted for the pixels identified as ice phase on the basis of the operational MODIS cloud product [22,23]. Ice clouds with optical thicknesses less than 0.3 have been considered as clear sky in the current MODIS

retrievals of cloud properties [37]. The same minimum threshold is also used for the retrieval in the present study. The retrieved optical thickness and effective particle size in the case of smooth surface are also shown in Figure 6. In general, the retrieved optical thicknesses associated with roughened ice crystals are smaller than the counterparts in the case of smooth particles, particularly, for the deep roughness condition (σ=1.00). This feature becomes more pronounced for ice clouds that are optically thick.

In the cases of slight and moderate roughness conditions (i.e., σ=0.001 and 0.10), the effect of surface roughness on the retrieved particle sizes is observed primarily for two effective radius regions of $r_e < 40\ \mu m$ or $r_e > 75\ \mu m$, where the retrieved radii associated with roughened particles are slightly smaller than their smooth surface counterparts. In the case of deep roughness condition (i.e., σ = 1.0), the effect of surface roughness on the retrieved effective size (r_e) is quite different for small and large particles. For small particles ($r_e < 35\ \mu m$), the effective sizes retrieved on the basis of the optical properties of roughened ice crystals are smaller than those based on the optical properties of smooth particles. This feature is consistent with that associated with slight or moderate roughness condition. For large particles ($r_e > 50\ \mu m$), the effective radii retrieved for deeply roughened (σ =1.0) particles are much larger than their counterparts for smooth ice crystals. For ice crystals with effective radii between 35 μm and 50 μm, the effect of surface roughness can lead either an overestimation or an underestimation in the retrieval of the effective particle size when the surfaces of ice crystals are deeply rough. This complicated feature of the impact of surface roughness on retrieving effective particle size of moderate ice crystals is not clear at this point and deserves a further investigation.

Figure 7 shows the histogram distributions of the retrieved ice cloud optical thicknesses and effective particle sizes associated with smooth and roughness conditions, which correspond to the results shown in Fig.6. In the case of the retrieved optical thicknesses, the relative distributions for σ=0, 0.01 and 0.1 are quite similar, which however are substantially different from that for σ=1.0. Specifically, the maximum of the distribution for σ=1.0 is observed at a smaller optical thickness in comparison with those in other three cases (i.e., σ=0.0, 0.01, and 0.1). It is evident from the overall patterns of the histogram distributions of the retrieved optical thicknesses, a deep surface roughness condition (e.g., σ=1.0) systematically leads to smaller values of the retrieved cloud optical thickness, particularly for thick clouds ($\tau > 5$).

The histogram distributions of the retrieved effective particle radii are quite similar for three roughness conditions, σ=0.0, 0.01, and 0.1. However, the histogram distribution of the retrieved effective particle radii in the case of σ=1.0 is systematically shifted towards larger particle sizes in comparison with the results for the other three cases. The results in Fig. 7 illustrate that the dominant effect of surface roughness associated with deeply roughened particles on the retrievals of ice cloud properties is to decrease optical thickness and to increase effective particle size. These results are consistent with the finding reported by Rolland et al. [7].

4. Summary and conclusions

Ice crystals in the atmosphere may have rough surfaces. The various surface roughness conditions could alter the single-scattering properties, thereby influencing the bulk scattering properties used for satellite-based retrieval of ice cloud properties. This

study investigated the influence of ice crystal roughness on the retrievals of ice cloud optical thickness and effective particle size.

A parameter describing the degree of ice crystal surface roughness is specified in computing the single-scattering properties of ice crystals. The single-scattering properties of hexagonal columns with different ice crystal surface roughness conditions have been averaged over particle size distributions to obtain the bulk scattering properties of ice clouds. The scattering properties show different features for different roughness conditions. With increasing roughness, the differences between the scattering properties of smooth and roughened ice crystals increase. Look-up tables based on the bidirectional reflectance at wavelengths 0.86 and 2.13 μm have been used to retrieve ice cloud optical thickness and effective particle size for cirrus clouds over oceans. In the case of slight or moderate roughness condition, the retrieved optical thicknesses and effective radii for roughened ice particles are not substantially different from their counterparts for smooth ice crystals. However, in the case of deep roughness condition, the dominant effect of surface roughness is to decrease the values of the retrieved cloud optical thickness and to increase the values of the retrieved effective particle size in comparison with the counterparts for smooth ice crystals.

These results have important implications for satellite remote sensing of cirrus clouds using visible/near-infrared channel data. Comparisons of cirrus cloud optical depths derived from surface or aircraft-based radar, lidar, and radiometer data show that the retrievals based on smooth crystal models tend to overestimate the cloud optical depth [38-40], but not necessarily the ice water path [39], which is proportional to the product of the optical depth and effective particle size. These overestimates of optical depth can

also cause underestimates of thin cirrus cloud-top heights because the 11-μm brightness temperature, used to obtain the true cloud temperature and height, emissivity depends on the cloud visible optical depth [41]. The smooth ice crystal models used by the MODIS operational (Collection 5) algorithm have asymmetry values at 0.66 μm ranging from 0.78 – 0.88 [42], while those used by the Clouds and the Earth's Radiant Energy System (CERES) project to analyze MODIS data [43] vary from 0.77 to 0.85 [40]. In situ observations indicate average values of g close to 0.76 [44,45]. Such small asymmetry parameters are difficult to obtain without surface roughness. Thus, by using roughened crystal models in the MODIS and CERES retrieval algorithms, it should be possible retrieve smaller optical depths and, in many cases, larger particle sizes. The smaller optical depths should yield better estimates of the true cloud temperature, while the ice water paths should remain virtually unchanged because the increased particle size will tend to offset the decreased optical depth. These new ice crystal scattering models have the potential for significantly reducing errors in many cirrus cloud retrievals. Further testing of the roughened ice crystal models in the operational retrieval codes is needed to verify whether the expected improvements can actually be realized.

Acknowledgements

Ping Yang's research is supported by the National Science Foundation Physical Meteorology Program (ATM-0239605), and a research grant (NNL06AA23G) from the National Aeronautics and Space Administration (NASA). George Kattawar's research is supported by the Office of Naval Research under contracts N00014-02-1-0478 and

N00014-06-1-0069. Patrick Minnis is supported through the NASA Radiation Sciences Program and the NASA Clouds and the Earth's Radiant Energy System Project.

References

[1] M. I. Mishchenko, W. B. Rossow, A. Macke, and A. A. Lacis, "Sensitivity of cirrus cloud albedo, bidirectional reflectance and optical thickness retrieval accuracy to ice particle shape," *J. Geophys. Res.,* vol. 101, no. D12, pp. 16 973-16 985, 1996.

[2] A. Macke, J. Mueller, and E. Raschke, "Single scattering properties of atmospheric ice crystal," *J. Atmos. Sci.,* vol. 53, no. 19, pp. 2813-2825, 1996a.

[3] P. Yang and K.-N. Liou, "Single-scattering properties of complex ice crystals in terrestrial atmosphere," *Contr. Atmos. Phys.,* vol. 71, no. 2, pp. 223-248, 1998.

[4] J. D. Cross, "Scanning electron microscopy of evaporating ice," *Science,* vol. 164. no. 3876, pp. 174–175, 1969.

[5] G. Davy, and D. Branton, "Subliming ice surfaces: Freeze-etch electron microscopy," *Science,* vol. 168, no. 3936, pp. 1216–1218, 1970.

[6] A. Ono, "The shape and riming properties of ice crystals in natural clouds," J. Atmos. Sci., vol. 26, pp. 138-147, 1969.

[7] P. Rolland, K.-N. Liou, M. D. King, S. C. Tsay, and G. M. McFarquhar, "Remote sensing of optical and microphysical properties of cirrus clouds using MODIS channels: methodology and sensitivity to assumptions," *J. Geophys. Res.,* vol. 105, no. D9, pp. 11 721-11 738, 2000.

[8] A. A. Kokhanovsky, and T. Nauss, "Satellite based retrieval of ice cloud properties using semianalytical algorithm," *J. Geophys. Res.,* vol. D110, D19206, doi: 10.1029/2004JD005744, 2005.

[9] H. Chepfer, G. Brogniez, and Y. Fouquart, "Cirrus clouds microphysical properties

deduced from POLDER observations," *J. Quant. Spectro. Radiat. Transfer*, vol. 60, no. 3, 375-390, 1998.

[10] H. Chepfer, P. Minnis, D. F. Young, L. Nguyen, and R. F. Arduini, "Estimation of cirrus cloud effective ice crystal shapes using visible reflectances from dual-satellite measurements," *J. Geophys. Res.,* vol. 107, 10.1029/2000JD000240, 2002.

[11] T. Inoue, "On the temperature and effective emissivity determination of semi-transparent cirrus clouds by bispectral measurements in the 10 microns window region," *J. Meteorology. Soc. Japan,* vol. 63, pp. 88-99, 1985.

[12] P. Minnis, Y. Takano, and K.-N. Liou, "Inference of cirrus cloud properties using satellite-observed visible and infrared radiances, Part I: Parameterization of radiance fields," *J. Atmos. Sci.,* vol. 50, no. 9, pp. 1279–1304, 1993.

[13] P. Minnis, P. W. Heck, and D. F. Young, "Inference of cirrus cloud properties using satellite-observed visible and infrared radiances, Part II: Verification of theoretical cirrus radiative properties," *J. Atmos. Sci.,* vol. 50, no. 9, pp. 1305–1322, 1993.

[14] M. D. King, W. P. Menzel, Y. J. Kaufman, D. Tanre, B.-C. Gao, S. Platnick, S. A. Ackerman, L. A. Remer, R. Pincus, and P. A. Hubanks, "Cloud and aerosol properties, precipitable water, and profiles of temperature and humidity from MODIS," *IEEE Trans. Geosci. Remote Sens.,* vol. 41, no. 2, pp. 442–458, 2003.

[15] K. Meyer, P. Yang, and B.-C. Gao, 2004: Optical thickness of tropical cirrus clouds derived from the MODIS 0.66 and 1.38-um channels. *IEEE Trans. Geosci. Remote Sens.* 42, 833-841.

[16] M. Chiriaco, H. Chepfer, V. Noel, A. Delaval, M. Haeffelin, P. Dubuisson, and P. Yang, "Improving retrievals of cirrus cloud particle size coupling lidar and three-

channel radiometric techniques," *Mon. Wea. Rev.,* vol. 132, no. 7, pp. 1684-1700, 2004.

[17] A. J. Baran, J. S. Foot, and D. L. Mitchell, "Ice-crystal absorption: A comparison between theory and implications for remote sensing," Appl. Opt., vol.37, no. 12, pp. 2207-2215 1998.

[18] G. Hong, P. Yang, H.-L. Huang, B. A. Baum, Y. X. Hu, and S. Platnick, "The sensitivity of ice cloud optical and microphysical passive satellite retrievals to cloud geometrical thickness," *IEEE Tran. Geosci. Remote Sens.,* vol. 45, no. 5, pp. 1315–1323, 2007.

[19] C. J. Stubenrauch, R. Holz, A. Chédin, D. L. Mitchell, A. J. Baran, "Retrieval of cirrus ice crystal sizes from 8.3 and 11.1 μm emissivities determined by the improved initialization inversion of TIROS-N Operational Vertical Sounder observations," *J. Geophys. Res.,* vol. 104, no. D24, pp. 31 793-31 808, 1999.

[20] Q. Fu and W. Sun, "Retrieval of cirrus particle sizes using a split-window technique: a sensitivity study," *J. Quant. Spectro. Radiat. Transfer*, vol 70, no. 4-6, pp. 725-736, 2001.

[21] T. Nakajima and M. D. King, "Determination of the optical thickness and effective particle radius of clouds from reflected solar radiation measurements. Part I: Theory," *J. Atmos. Sci.,* vol. 47, no. 5, pp. 1878–1893, 1990.

[22] M. D. King, W. P. Menzel, Y. J. Kaufman, D. Tanré, B. C. Gao, S. Platnick, S. A. Ackerman, L. A. Remer, R. Pincus, and P. A. Hubanks, "Cloud and aerosol properties, precipitable water, and profiles of temperature and humidity from MODIS," *IEEE Trans. Geosci. Remote Sens.,* vol. 41, no. 2, pp. 442–458, 2003.

[23] S. Platnick, M. D. King, S. A. Ackerman, W. P. Menzel, B. A. Baum, J. C. Riédi, and R. A. Frey, "The MODIS cloud products: Algorithms and examples from Terra," *IEEE Trans. Geosci. Remote Sens.,* vol. 41, no. 2, pp. 459–473, 2003.

[24] M. D. King, S. Platnick, P. Yang, G. T. Arnold, M. A. Gray, J. C. Riédi, S. A. Ackerman, and K. N. Liou, "Remote sensing of liquid water and ice cloud optical thickness, and effective radius in the arctic: Application of air-borne multispectral MAS data," *J. Atmos. and Ocean. Technol.,* vol. 21, no. 6, pp. 857–875, 2004.

[25] B. A. Baum, A. J. Heymsfield, P. Yang, and S. T. Bedka, "Bulk scattering properties for the remote sensing of ice clouds. Part I: Microphysical data and models," *J. Appl. Meteor.,* vol. 44, pp. 1885–1895, 2005.

[26] P. Yang, G. Hong, G. W. Kattawar, P. Minnis and Y. Hu, "Uncertainties with the surface of ice particles in satellite-based retrieval of cirrus clouds: Part I. Single-scattering properties of ice crystals with surface roughness, *IEEE Tran. Geosci. Remote Sens., (submitted)*

[27] C. Cox and Munk, W., "Measurement of the roughness of the sea surface from photographs of the sun's glitter," *J. Opt. Amer. Soc.,* vol. 44, no. , pp. 838-850, 1954.

[28] V. Shcherbakov, J.-F. Gayet, B. Baker, and P. Lawson, "Light scattering by single natural ice crystals," *J. Atmos. Sci.*, vol. 63, no. 5, 1513–1525, 2006.

[29] A. Macke and M. I. Mishchenko, "Applicability of regular particle shapes in light scattering calculations for atmospheric ice particles," *Appl. Opt.*, vol. 35, no. 21, 4291-4296, 1996.

[30] T. C. Grenfell, S. P. Neshyba, and S. G. Warren, "Representation of a nonspherical ice particle by a collection of independent spheres for scattering and absorption of radiation: 3. Hollow columns and plates," *J. Geophys. Res.*, vol. 110, D17203, doi:10.1029/2005JD005811, 2005.

[31] Q. Fu, "Generalized parameterization of asymmetry factor of cirrus clouds for climate models," *J. Atmos. Sci.,* (accepted), 2007.

[32] P. Yang, K. N. Liou, K. Wyser, and D. Mitchell, "Parameterization of the scattering and absorption properties of individual ice crystals," *J. Geophys. Res.,* vol. 105, no. D4, pp. 4699-4718, 2000.

[33] J. E. Hansen and L.D. Travis, "Light scattering in planetary atmospheres," *Space. Sci. Rev.,* vol. 16, no. 4, pp. 527-610, 1974.

[34] P. Yang and K. N. Liou, "Geometric-optics-integral-equation method for light scattering by nonspherical ice crystals," *Appl. Opt.,* vol. 35, no. 33, pp. 6568-6584, 1996b.

[35] A. L. Kosarev and I. P. Mazin, "An empirical model of the physical structure of upper layer clouds," *Atmos. Res.,* vol. 26, no. 3, pp. 213–228, 1991.

[36] B. A. Baum, P. Yang, A. J. Heymsfield, S. Platnick, M. D. King, Y. X. Hu, and S. T. Bedka, "Bulk scattering properties for the remote sensing of ice clouds. Part II: Narrowband models," *J. Appl. Meteor.,* vol. 44, pp. 1896–1911, 2005.

[37] A. E. Dessler and P. Yang, "The distribution of tropical thin cirrus clouds inferred from Terra MODIS data," *J. Climate,* vol. 16, no. 8, pp. 1241–1247, 2003.

[38] Q. Min, P. Minnis, and M. M. Khaiyer, "Comparison of cirrus optical depths from GOES-8 and surface measurements," *J. Geophys. Res.*, vol. 109, no. D15207, D20119, 10.1029/2003JD004390, 2004.

[39] G. G. Mace, Y. Zhang, S. Platnick, M. D. King, P. Minnis, and P. Yang, "Evaluation of cirrus cloud properties from MODIS radiances using cloud properties derived from ground-based data collected at the ARM SGP site," *J. Appl. Meteorol.*, vol. 44, no. 2, 221-240, 2005.

[40] M. Chiriaco, H. Chepfer, P. Minnis, M. Haeffelin, S. Platnick, D. Baumgardner, P. Dubuisson, M. McGill, V. Noel, J. Pelon, D. Spangenberg, S. Sun-Mack, and G. Wind, "Comparison of CALIPSO-like, LaRC, and MODIS retrievals of ice cloud properties over SIRTA in France and Florida during CRYSTAL-FACE," *J. Appl. Meteorol. Climatol.*, vol. 46, no.3, 249-272, 2007.

[41] P. Minnis, D. P. Garber, D. F. Young, R. F. Arduini, and Y. Takano, "Parameterization of reflectance and effective emittance for satellite remote sensing of cloud properties," *J. Atmos. Sci.*, vol. 55, no. 22, 3313-3339, 1998.

[42] B. A. Baum, P. Yang, A. J. Heymsfield, S. Platnick, M. D. King, Y.-X. Hu, and S. T. Bedka, 2005: Bulk scattering models for the remote sensing of ice clouds. Part 2: Narrowband models. *J. Appl. Meteor.*, vol. 44, no. 12, pp. 1896-1911.

[43] P. Minnis, D. P. Kratz, J. A. Coakley, Jr., M. D. King, D. Garber, P. Heck, S. Mayor, D. F. Young, and R. Arduini, "Cloud Optical Property Retrieval (Subsystem 4.3). 'Clouds and the Earth's Radiant Energy System (CERES) Algorithm Theoretical Basis Document, Volume III: Cloud Analyses and Radiance Inversions (Subsystem 4)'", *NASA RP 1376 Vol. 3*, edited by CERES Science Team, pp. 135-176, 1995.

[44] H. Gerber, H., Y. Takano, T. J. Garrett, and P. V. Hobbs, "Nephelometer measurements of the asymmetry parameter, volume extinction coefficient, and backscatter ratio in clouds," *J. Atmos. Sci.*, vol. 57, no. 18, 3021–3034, 2000.

[45] T. J. Garrett, T. J., H. Gerber, D. G. Baumgardner, C. H. Twohy, and E. M. Weinstock, "Small, highly reflective ice crystals in low-latitude cirrus," *Geophys. Res. Lett.*, vol. 30, no. 21, doi:10.1029/2003GL018153, 2003.

Figure Captions

Fig. 1. The probability density function, $\xi(z_\alpha, z_\beta)$, for the spatial orientations of the rough surface facets of an ice crystal. The parameters z_α and z_β indicate the slopes of a facet of the roughened surface along two orthogonal directions. To avoid using a 3D illustration, here $\xi(z_\alpha, z_\beta)$ is plotted versus z_α in the case of $z_\beta = 0$.

Figure 2. The phase functions at a wavelength of 0.66 μm for randomly oriented hexagonal ice crystals with three different surface roughness conditions. The refractive index at wavelength 0.66 μm is $1.3078 + i1.66 \times 10^{-8}$.

Figure 3. Comparison of the asymmetry factors as functions of particle aspect ratio for various roughness conditions. The wavelength and refractive used in the computation are 0.66 μm and $1.3078 + i1.66 \times 10^{-8}$, respectively. To specify ice crystal sizes, the surface areas of ice crystals are defined as the same as that of an ice crystal with $a/L = 60\mu m / 300\mu m$.

Figure 4. Asymmetry factors as function of maximum dimensions of column with four different surface roughness conditions σ = 0.00, 0.01, 0.10, and 1.00. The aspect ratio is 2a/L = 1/3. The wavelength and refractive used in the computation are 0.66 μm and $1.3078 + i1.66 \times 10^{-8}$, respectively.

Figure 5. Comparisons of phase functions at 0.86- and 2.13-μm for different surface roughness conditions, σ = 0.00, 0.01, 0.10, and 1.00 with an effective particle radius of 30-μm. Comparisons of built lookup tables using 0.86- and 2.13-μm reflectances for different surface roughness conditions, σ = 0.00, 0.01, 0.10, and 1.00 with a solar zenith angle of 30°, a satellite zenith angle of 0°, and a relative azimuth angle of 90°.

Figure 6. Upper panels: MODIS L1B granule image (RGB=band 4:3:1), the retrieved ice cloud optical thicknesses, and effective particle sizes (specifically, effective radii defined on the basis of Eq. 5) with roughness σ = 0.00. Middle panels: the comparisons of retrieved ice cloud optical thicknesses from different roughness conditions, σ = 0.00, 0.01, 0.10, and 1.00. Bottom panels: the comparisons of retrieved ice cloud effective particle sizes from different roughness conditions: σ = 0.00, 0.01, 0.10, and 1.00.

Figure 7. Histogram distributions of the retrieved ice cloud optical thicknesses and effective particle radii for four roughness conditions (σ = 0.00, 0.01, 0.10, and 1.00), which correspond to the results shown in Fig. 6.

Authors' Bio-Sketches

Ping Yang received the B.S. (theoretical physics) and M.S. (atmospheric physics) degrees from Lanzhou University and Lanzhou Institute of Plateau Atmospheric Physics, Chinese Academy of Sciences, Lanzhou, China, in 1985 and 1988, respectively, and the Ph.D. degree in meteorology from the University of Utah, Salt Lake City, USA, in 1995.

He is currently an Associate Professor in the Department of Atmospheric Sciences, Texas A&M University, College Station, Texas, USA. After graduation from the University of Utah, he remained there for two years, working as a Research Associate. Later, he was an Assistant Research Scientist at the University of California, Los Angeles, and an Associate Research scientist in the Goddard Earth Sciences & Technologies Center, University of Maryland Baltimore County. His research interests cover the areas of remote sensing and radiative transfer. He has been actively conducting research in the modeling of the optical and radiative properties of clouds and aerosols, in particular, cirrus clouds, and their applications to space-borne and ground-based remote sensing. He has co-authored more than 100 peer-reviewed publications. He received a best paper award from the Climate and Radiation Branch, NASA Goddard Space Center in 2000, the U.S. National Science Foundation CAREER award in 2003, and the Dean's Distinguished Achievement Award for Faculty Research, College of Geosciences, Texas A&M University in 2004. He is a member of the MODIS Science Team. He currently serves as an associate editor for the *Journal of Atmospheric Sciences*, the *Journal of Quantitative Spectroscopy & Radiative Transfer*, and the *Journal of Applied Meteorology and Climatology*.

Gang Hong received the B.S. degree in Atmospheric Sciences from Nanjing Institute of Meteorology, Nanjing, China in 1995 and the Ph.D. degree in Environmental Physics and Remote Sensing from the University of Bremen, Germany in 2004. Currently, he is a

Research Associate at the Department of Atmospheric Sciences, Texas A&M University. His recent research focuses on retrieving ice cloud and aerosol properties and investigating the radiative properties of clouds on the basis of the MODIS and AIRS measurements.

George W. Kattawar is presently a Professor of Physics at Texas A&M University in College Station, Texas where he also obtained his M.S. and Ph. D. degrees. He is the author/coauthor of over 120 publications in fields ranging from radiative transfer in atmosphere-ocean systems to quantum optics. His present research interests are in radiative transfer in realistic planetary atmospheres and oceans with inclusion of polarization and high resolution spectroscopic calculations such as Raman and Rayleigh-Brillouin scattering, Mueller matrix imaging in turbid media, and electromagnetic scattering from irregularly shaped objects.

Patrick Minnis is a senior research scientist in the Climate Sciences Branch, NASA Langley Research Center in Hampton, VA, where he has served for more than 25 years. He received a B.E. in materials science and metallurgical engineering at Vanderbilt University in 1972, a M.S. in Atmospheric Science from Colorado State University in 1978, and a Ph.D. in meteorology from the University of Utah (1991). His research is focused on the remote sensing of clouds and surface properties from satellite imagery for weather and climate investigations. He is the author/coauthor of over 150 peer-reviewed publications and has been awarded the NASA medals for Exceptional Scientific Achievement (1993) and Exceptional Achievement (2005) and the AMS Henry G. Houghton Award for Atmospheric Physics (1998). He is a member of the CERES, ARM, and ICESat Science Teams and leads a research group conducting analyses of polar-

orbiting and geostationary satellite data for field missions, operational aircraft icing condition diagnosis, and contrail research. He currently serves as an editor for the Journal of Atmospheric Sciences.

Yongxiang Hu received his Ph.D. in Atmospheric Sciences from University of Alaska, Fairbanks, USA, in 1994. He is currently a senior research scientist in the Climate Sciences Branch, NASA Langley Research Center in Hampton, VA. He worked as postdoctoral researcher at College of William and Mary, and as research professor at Hampton University before he joined NASA in 1999. His research interests include radiative transfer, passive and active atmospheric remote sensing and satellite onboard data analysis.

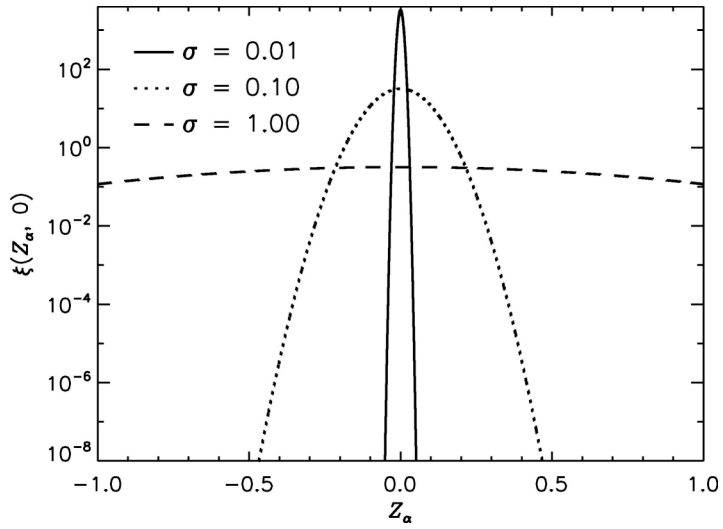

Fig. 1. The probability density function, $\xi(z_\alpha, z_\beta)$, for the spatial orientations of the rough surface facets of an ice crystal. The parameters z_α and z_β indicate the slopes of a facet of the roughened surface along two orthogonal directions. To avoid using a 3D illustration, here $\xi(z_\alpha, z_\beta)$ is plotted versus z_α in the case of $z_\beta = 0$.

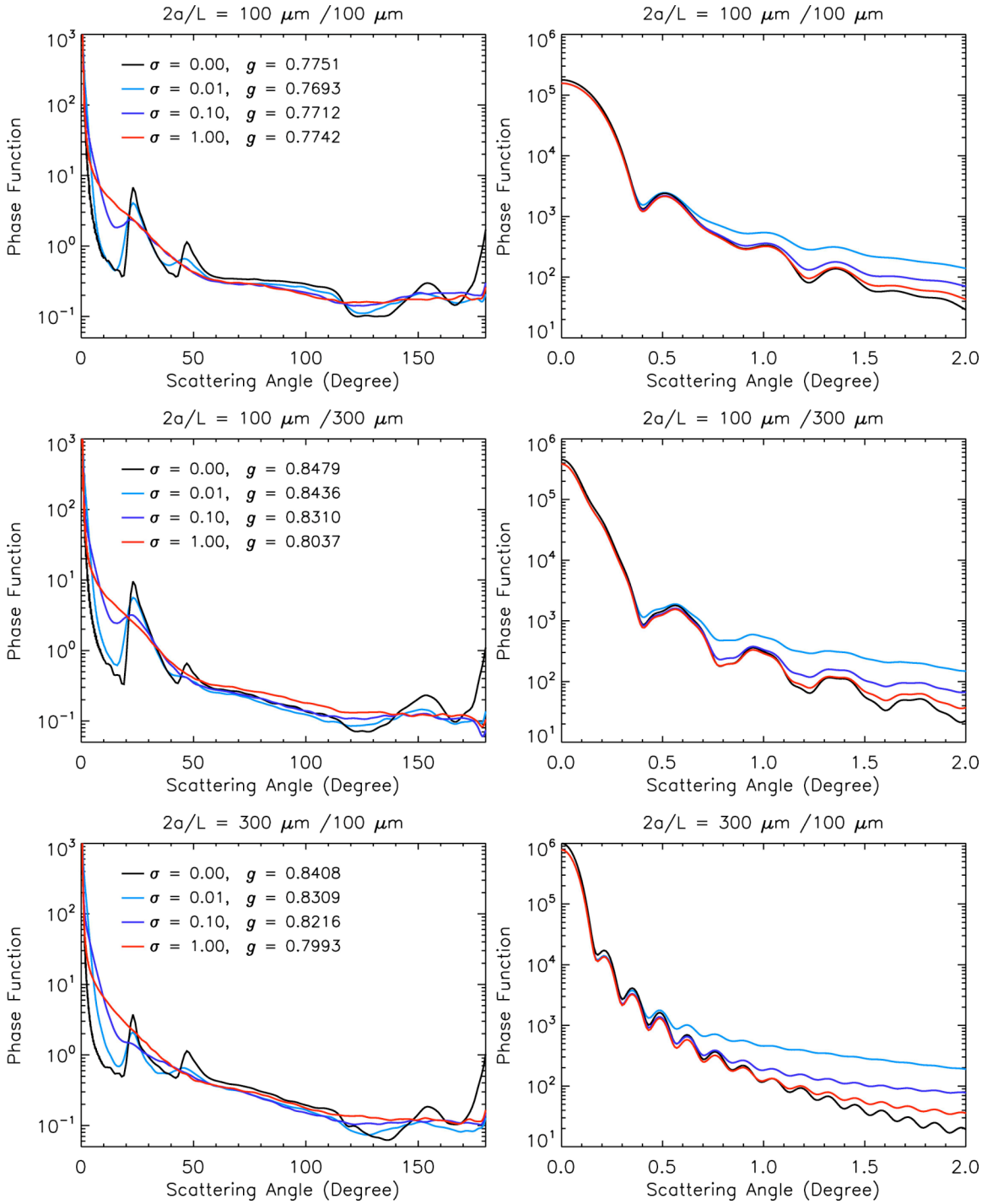

Figure 2. The phase functions at a wavelength of 0.66 μm for randomly oriented hexagonal ice crystals with three different surface roughness conditions. The refractive index at wavelength 0.66 μm is $1.3078 + i1.66 \times 10^{-8}$.

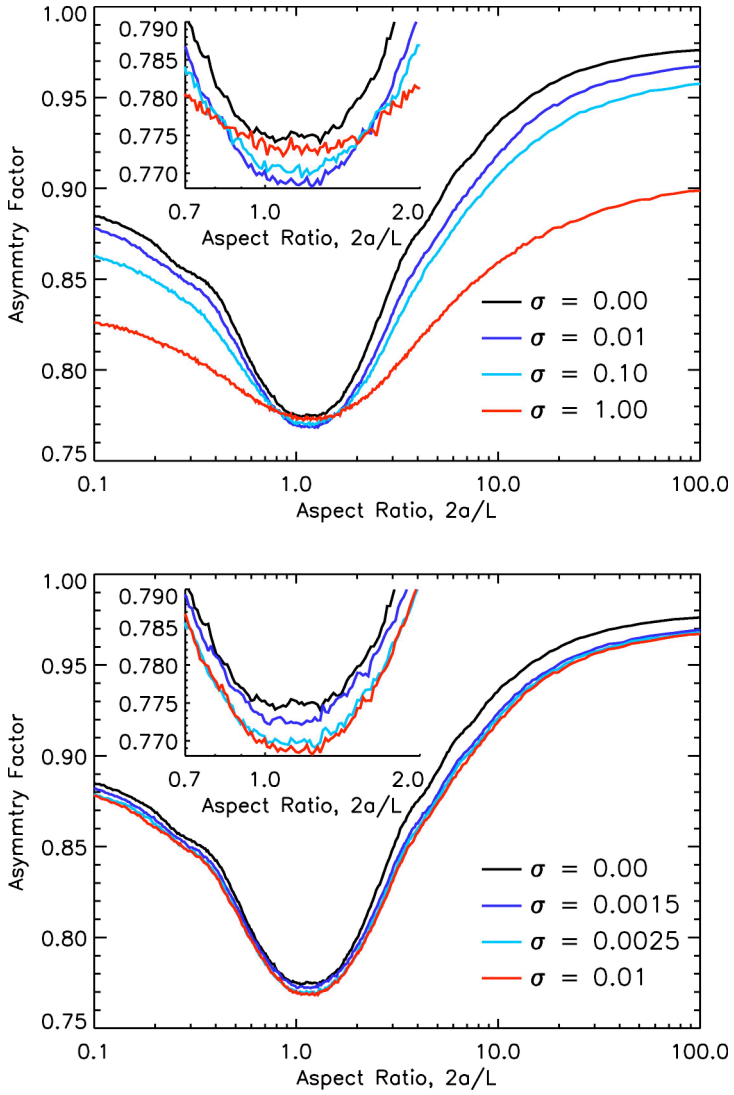

Figure 3. Comparison of the asymmetry factors as functions of particle aspect ratio for various roughness conditions. The wavelength and refractive used in the computation are 0.66 μm and $1.3078 + i1.66 \times 10^{-8}$, respectively. To specify ice crystal sizes, the surface areas of ice crystals are defined as the same as that of an ice crystal with $a/L = 60\mu m/300\mu m$.

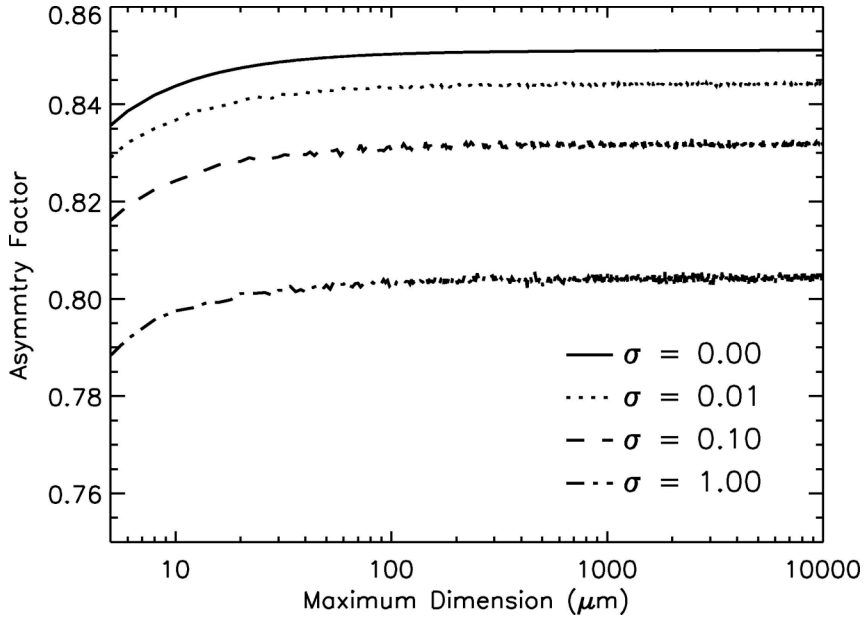

Figure 4. Asymmetry factors as function of maximum dimensions of column with four different surface roughness conditions σ = 0.00, 0.01, 0.10, and 1.00. The aspect ratio is 2a/L = 1/3. The wavelength and refractive used in the computation are 0.66 μm and $1.3078 + i1.66 \times 10^{-8}$, respectively.

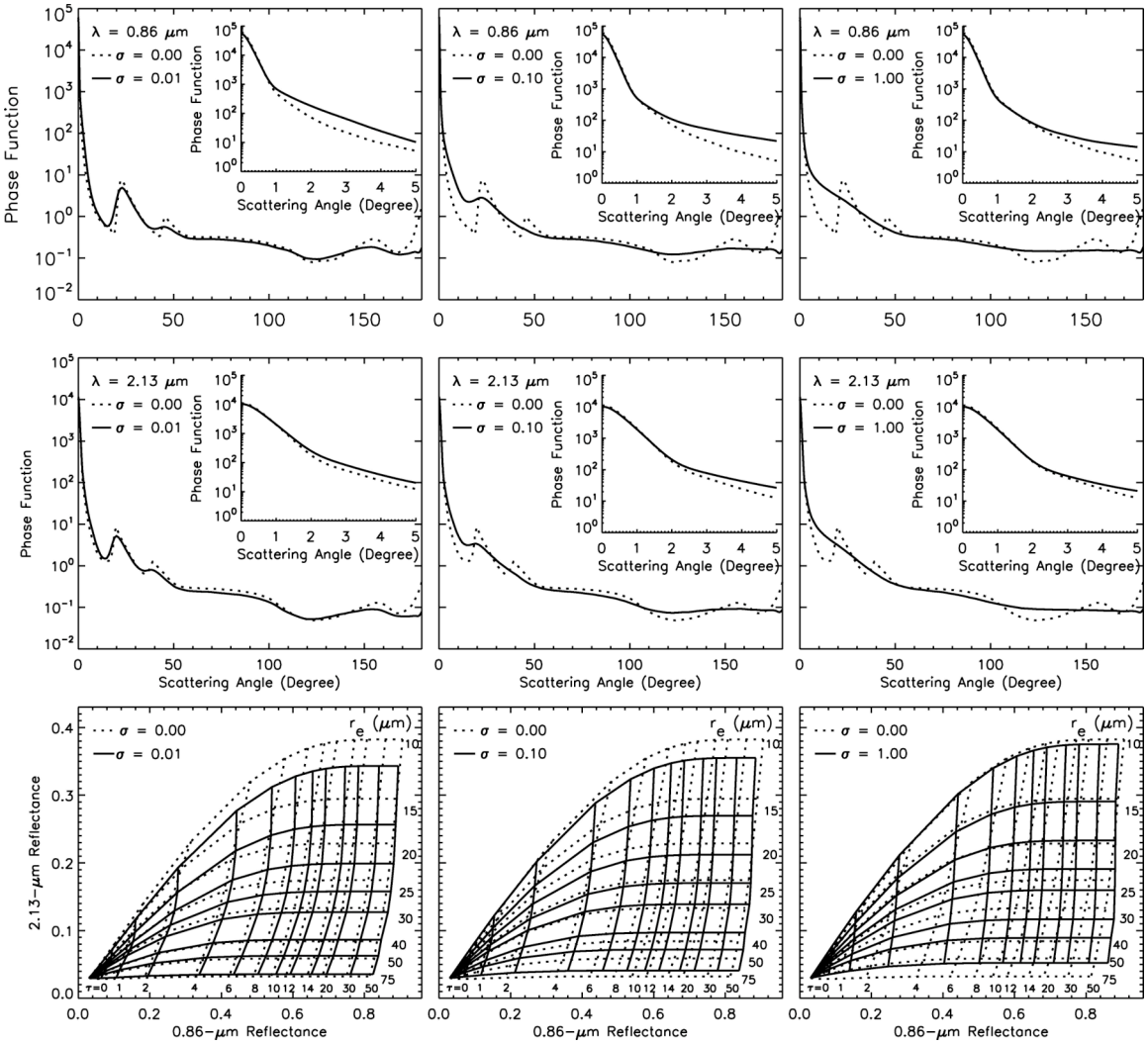

Figure 5. Comparisons of phase functions at 0.86- and 2.13-μm for different surface roughness conditions, σ = 0.00, 0.01, 0.10, and 1.00 with an effective particle radius of 30-μm. Comparisons of built lookup tables using 0.86- and 2.13-μm reflectances for different surface roughness conditions, σ = 0.00, 0.01, 0.10, and 1.00 with a solar zenith angle of 30°, a satellite zenith angle of 0°, and a relative azimuth angle of 90°.

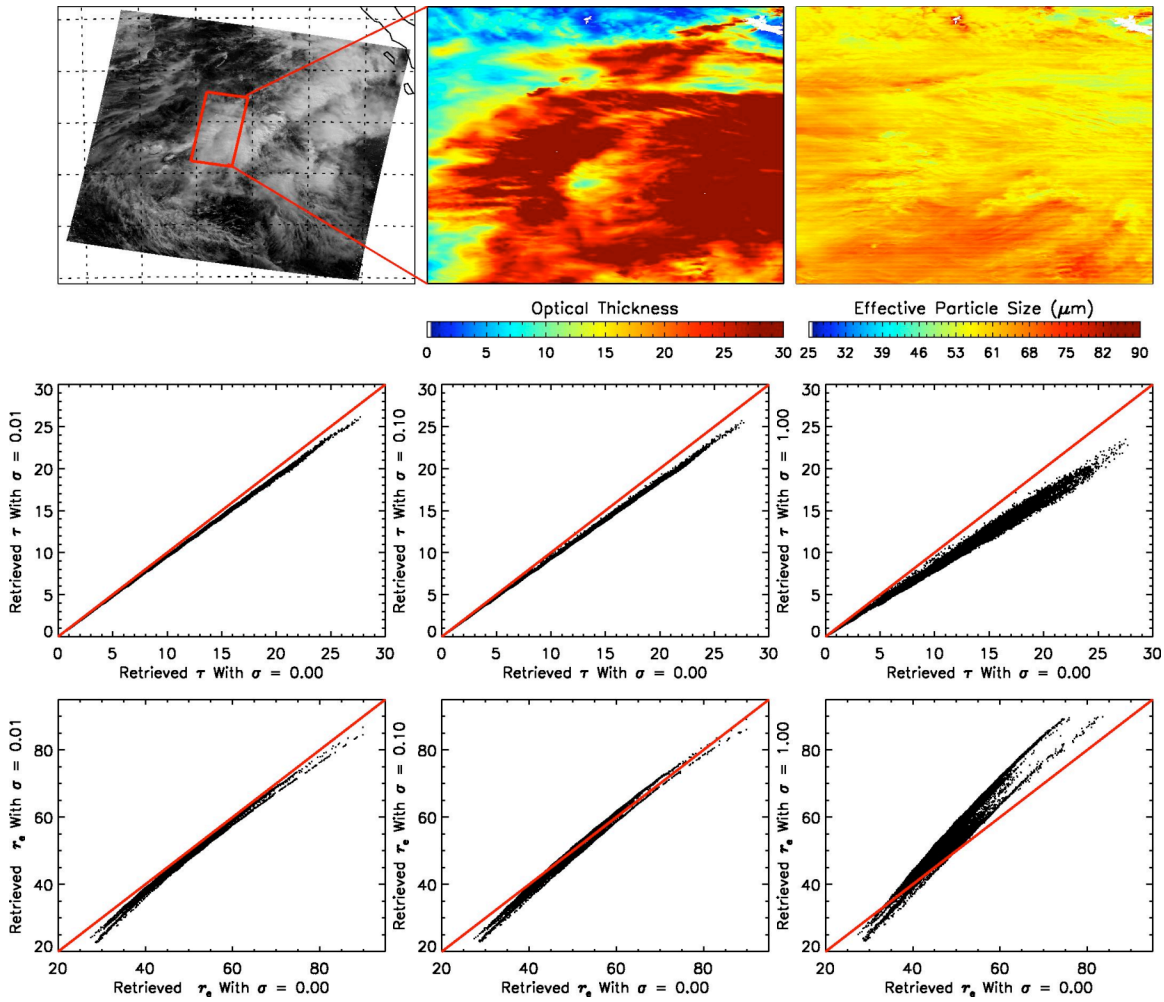

Figure 6. Upper panels: MODIS L1B granule image (RGB=band 4:3:1), the retrieved ice cloud optical thicknesses, and effective particle sizes (specifically, effective radii defined on the basis of Eq. 5) with roughness σ = 0.00. Middle panels: the comparisons of retrieved ice cloud optical thicknesses from different roughness conditions, σ = 0.00, 0.01, 0.10, and 1.00. Bottom panels: the comparisons of retrieved ice cloud effective particle sizes from different roughness conditions: σ = 0.00, 0.01, 0.10, and 1.00.

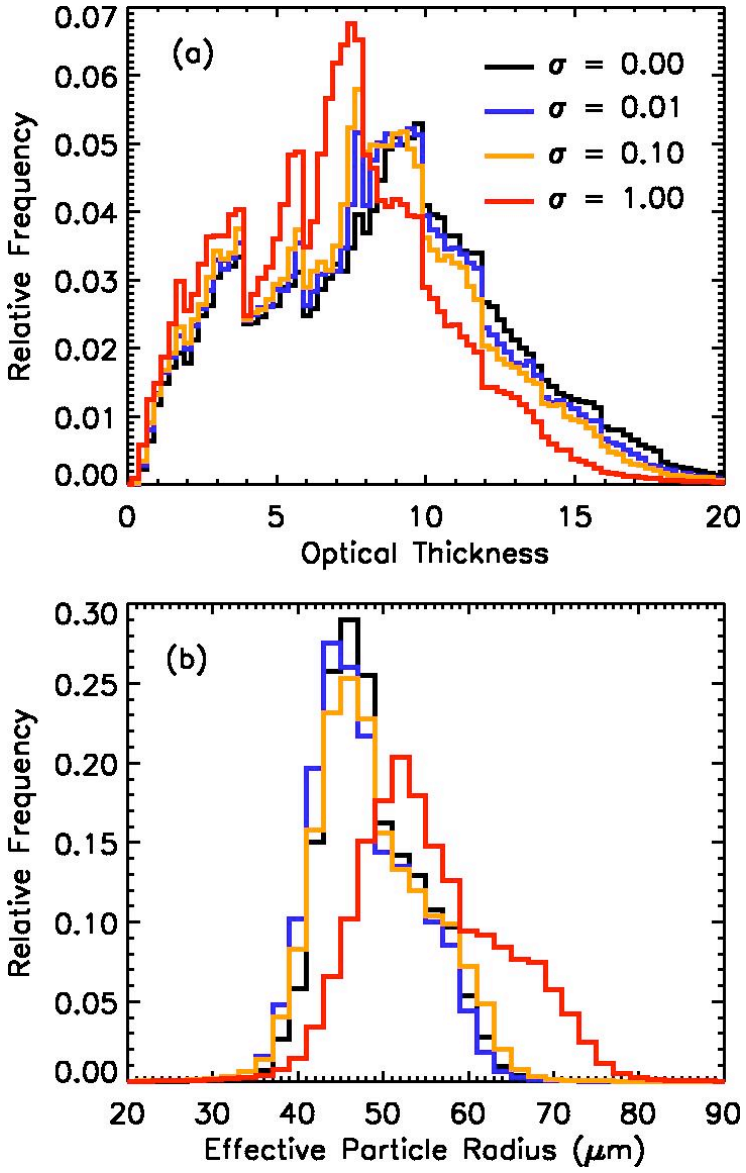

Figure 7. Histogram distributions of the retrieved ice cloud optical thicknesses and effective particle radii for four roughness conditions (σ = 0.00, 0.01, 0.10, and 1.00), which correspond to the results shown in Fig. 6.